

Room-temperature operation type-II GaSb/GaAs quantum-dot infrared light-emitting diode

Shih-Yen Lin, Chi-Che Tseng, Wei-Hsun Lin, Shu-Cheng Mai, Shung-Yi Wu, Shu-Han Chen, and Jen-Inn Chyi

Citation: *Applied Physics Letters* **96**, 123503 (2010); doi: 10.1063/1.3371803

View online: <http://dx.doi.org/10.1063/1.3371803>

View Table of Contents: <http://scitation.aip.org/content/aip/journal/apl/96/12?ver=pdfcov>

Published by the [AIP Publishing](#)

Articles you may be interested in

[InP-based 2.8–3.5 \$\mu\$ m resonant-cavity light emitting diodes based on type-II transitions in GaInAs/GaAsSb heterostructures](#)

Appl. Phys. Lett. **101**, 221107 (2012); 10.1063/1.4768447

[External efficiency and carrier loss mechanisms in InAs/GaInNAs quantum dot light-emitting diodes](#)

J. Appl. Phys. **108**, 033104 (2010); 10.1063/1.3467004

[Complex emission dynamics of type-II GaSb/GaAs quantum dots](#)

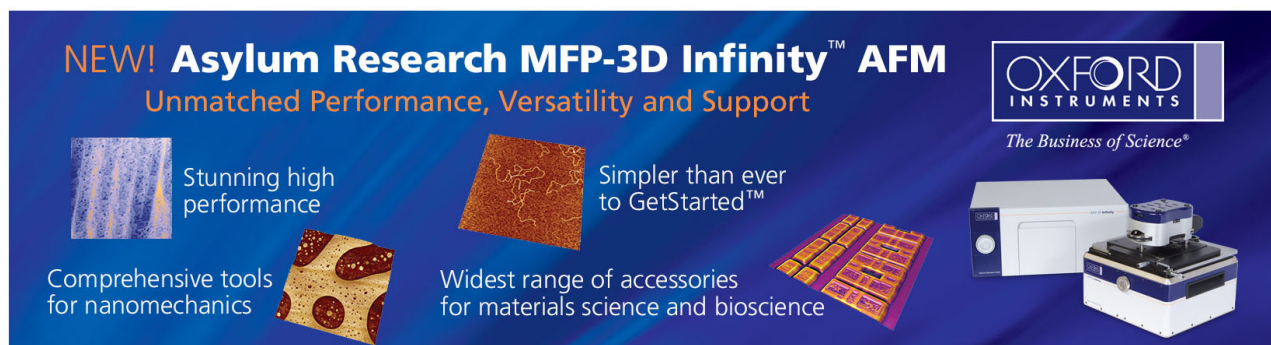
Appl. Phys. Lett. **95**, 061102 (2009); 10.1063/1.3202419

[Tunable interband and intersubband transitions in modulation C-doped In Ga As Ga As quantum dot lasers by postgrowth annealing process](#)

Appl. Phys. Lett. **93**, 071111 (2008); 10.1063/1.2968191

[Electrically injected InGaAs/GaAs quantum-dot microcavity light-emitting diode operating at 1.3 \$\mu\$ m and grown by metalorganic chemical vapor deposition](#)

Appl. Phys. Lett. **84**, 4155 (2004); 10.1063/1.1755411



NEW! Asylum Research MFP-3D Infinity™ AFM
Unmatched Performance, Versatility and Support

OXFORD INSTRUMENTS
The Business of Science®

Stunning high performance
Simpler than ever to GetStarted™

Comprehensive tools for nanomechanics
Widest range of accessories for materials science and bioscience

Room-temperature operation type-II GaSb/GaAs quantum-dot infrared light-emitting diode

Shih-Yen Lin,^{1,2,a)} Chi-Che Tseng,¹ Wei-Hsun Lin,¹ Shu-Cheng Mai,¹ Shung-Yi Wu,¹ Shu-Han Chen,¹ and Jen-Inn Chyi^{1,3}

¹Research Center for Applied Sciences, Academia Sinica, Taipei, Taiwan

²Department of Photonics, National Chiao-Tung University, Hsinchu, Taiwan and Institute of Optoelectronic Sciences, National Taiwan Ocean University, Keelung, Taiwan

³Department of Electrical Engineering, National Central University, Zhongli, Taiwan

(Received 10 December 2009; accepted 3 March 2010; published online 23 March 2010)

A GaSb/GaAs quantum-dot light-emitting diode (QD LED) with a single GaSb QD layer is investigated in this paper. The room-temperature photoluminescence peak blueshift with increasing excitation power densities suggests a type-II alignment of the GaSb/GaAs heterostructures. Significant electroluminescence (EL) is observed for the device under forward biases, which suggests that pronounced dipole transitions occur at the GaSb/GaAs interfaces. With increasing forward biases, the observed EL peak blueshift confirms that the origin of luminescence is from the type-II GaSb/GaAs QD structures. A model is established to explain the operation mechanisms of the type-II QD LED. © 2010 American Institute of Physics. [doi:10.1063/1.3371803]

Two possible transition mechanisms are adopted for optoelectronic devices based on the InAs/GaAs quantum-dot (QD) structures, which are (a) interband and (b) intraband transitions in the QD structures. The representative device for the interband transition is the near infrared QD laser diode (LD), while QD infrared photodetectors (QDIPs) is for the intraband transition.¹⁻⁴ Although great performances have already been observed for the two devices, difficulties like longer emitting wavelengths up to 1.55 μm and 3–5 μm detections are still remained for QD LDs and QDIPs, respectively. For the long-wavelength QD LDs, attempts like InGaAs capping layers grown after InAs QDs and Sb-incorporation in the capping layers are already demonstrated.^{5,6} Although enhanced emitting wavelengths are obtained for these structures, reliable device performances are still unavailable. The main reason responsible for the emitting wavelength limitation of QD LDs is the limited choice of barriers like GaAs and InGaAs layers. In previous reports, despite its type-II alignment, photoluminescence (PL) has already been observed for GaSb/GaAs QDs.^{7,8} The main advantage of the GaSb QD structure is the wide barrier choice from GaAs to GaAsSb and even InGaP. The choice of different barriers may provide different emitting wavelengths for the devices based on this QD structure.

In this paper, a single GaSb QD layer with optimized growth conditions is inserted in a GaAs n-i-p diode structure. The room-temperature PL peak blueshift with increasing excitation power densities suggests a type-II alignment of the GaSb/GaAs heterostructure. The linear dependence of the PL peak energies over the third root of laser power densities is also observed, which confirms that the luminescence is from the type-II GaSb/GaAs QDs.⁹ Significant electroluminescence (EL) is observed for the device under forward biases, which suggests that pronounced dipole transitions occur at the GaSb/GaAs interfaces. With increasing forward biases, the observed EL peak blueshift confirms that the origin of luminescence is from the type-II GaSb/GaAs QD structures.

The results have demonstrated that by optimizing the growth conditions, the influence of group-V interfaces is greatly depressed. The accumulation of holes and electrons at the GaSb/GaAs interfaces has enhanced the dipole transition probability such that significant EL could be observed for the type-II GaSb QD light-emitting diode (LED).

The GaSb QD LED sample discussed in this paper is prepared by Riber Compact 21 solid-source molecular beam epitaxy system. With (100)-oriented semi-insulating GaAs substrate, a single 3.0 monolayer (ML) GaSb QD layer are embedded in the GaAs n-i-p structure. The growth procedure for the sample is (a) a 300 nm GaAs bottom contact layer p-type doped to $2 \times 10^{18} \text{ cm}^{-3}$ grown at 580 °C, (b) a 200 nm undoped GaAs layer grown at 580 °C, (c) a 3.0 ML GaSb QD layer grown at 490 °C with V/III ratio ~ 1.3 , (d) a 200 nm undoped GaAs layer grown at 580 °C and (e) a 300 nm GaAs top contact layer n-type doped to $2 \times 10^{18} \text{ cm}^{-3}$ grown at 580 °C. Since severe As/Sb exchange at the GaSb/GaAs interfaces has been reported elsewhere, pre- and post-Sb soaking procedures with 15 and 120 s durations during GaSb QD growth are adopted to protect the GaSb QD structure.¹⁰ Standard photolithography and wet chemical etching are adopted to fabricate the devices with $450 \times 630 \mu\text{m}^2$ mesas. For light extraction, grid top contact is adopted. The positive and negative biases of the measurements are defined according to the voltages applied to the bottom contact of the device. The Keithley 6487 system is used to measure current-voltage (I-V) characteristics and acts as the voltage source. The PL and EL spectrums are measured by using Jobin Yvon's NanoLog3 system coupled with a He-Ne laser as the pumping source.

The room-temperature PL spectrums of the sample measured under different pumping power densities 0.38, 0.59, and 0.95 W/cm^2 are shown in Fig. 1(a). As shown in the figure, with increasing pumping power densities, the PL peak would shift from 1.085 to 1.102 eV. The PL peak blueshift with increasing pumping power is frequently observed for type-II heterostructures.¹¹ Due to the spatial separation of electron/hole confinements of the type-II GaSb/GaAs QDs,

^{a)}Electronic mail: shihyen@gate.sinica.edu.tw.

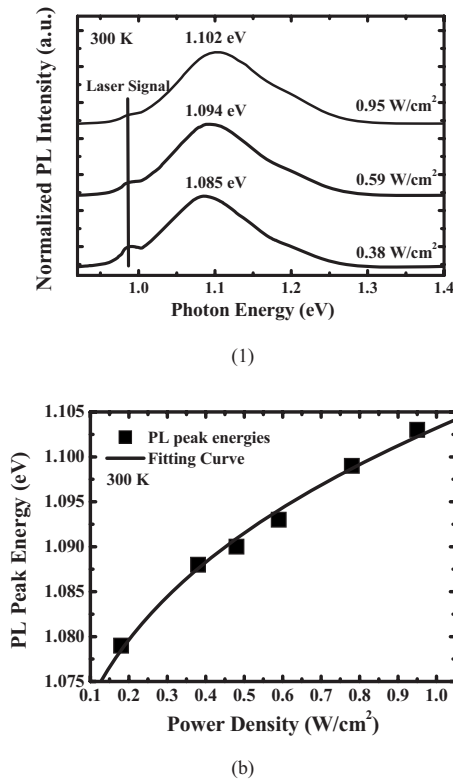


FIG. 1. (a) The room-temperature PL spectrums of the sample measured under different pumping power densities 0.38, 0.59, and 0.95 W/cm^2 . The peak at ~ 0.98 eV ($1.265 \mu\text{m}$) is resulted from the excitation laser (632.8 nm). (b) The PL peak energies obtained under different excitation powers and the fitting curve of the peaks with the third root of the excitation densities.

the accumulation of electron/hole at the GaAs/GaSb interfaces with increasing pumping power density would steepen the band bending near the interface. In this case, upraised confinement states in the GaAs triangular wells would result in a PL peak blueshift as shown in the figure. The other supporting evidence of the type-II luminescence is the linear dependence of the PL peak energies over the third root of the excitation density.⁹ The PL peak energies measured under different power densities at room temperature are shown in Fig. 1(b). As shown in the figure, the fitting curve (PL peak energy) = $1.04648 + 0.05673 \times (\text{power density})^{1/3}$ shows good agreement with the experimental results. The increase in PL peak energies with increasing excitation densities and their linear dependence over the third root of the excitation density have confirmed that the PL signals are from the type-II GaSb/GaAs QDs.

The I-V characteristics of the device at room temperature are shown in Fig. 2(a). The inset in the figure shows the top view of the device. As shown in the figure, the leakage currents of the device under reverse biases are below 10^{-7} A, which suggests a good P-N junction. The turn-on voltage of the device is at 0.8 V. The room-temperature EL spectrums of the device under 1.0, 1.5, and 2.0 V are shown in Fig. 2(b). For applied voltages lower than 0.8 V, no luminescence is observed for the device. Considering the turn-on voltage of the device is at 0.8 V, the results suggest that as long as the device turns on, optical recombination would take place immediately. The EL peaks measured under different current densities with forward biases 0.8 to 2.5 V are shown in the inset of Fig. 2(b). Since a voltage source is

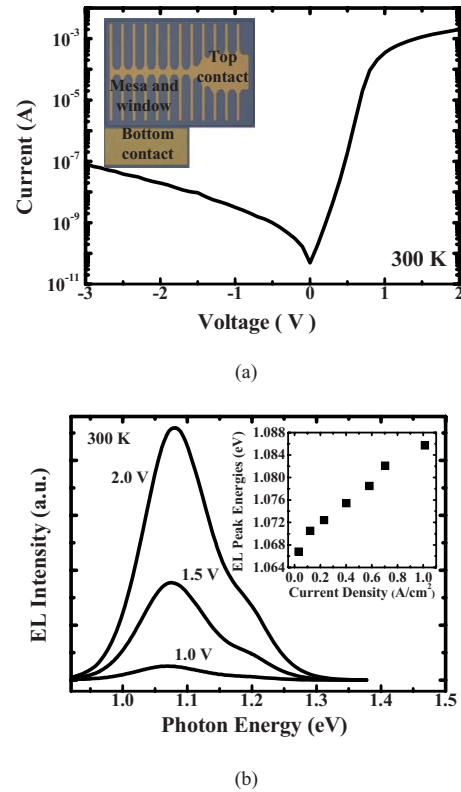


FIG. 2. (Color online) (a) The I-V characteristics and (b) the room-temperature EL spectrums of the device. The applied voltages for the EL spectrums are 1.0, 1.5, and 2.0 V, respectively. The inset figure in (b) shows the EL peak energies of the device under different injection current densities.

adopted for EL measurements, the current densities are extracted from the I-V curve of the device shown in Fig. 2(a). As shown in the figure, EL peak blueshift from 1.067 to 1.086 eV is observed with increasing injection current density. The results are consistent with the observation of PL peak blueshift with increasing excitation laser powers, which suggests that the type-II GaSb/GaAs QD structure should be responsible for the EL spectrum.

To further investigate if the EL and PL signals are from the same mechanism, it is helpful to see if the fitting equation of PL peak energies could be applied to EL peak energies. Compared with PL measurements, to obtain similar peak energy 1.08 eV of the device operated at 2.0 V ($0.71 \text{ A}/\text{cm}^2$), the excitation laser power density of the PL measurement has to be decreased down to $0.18 \text{ W}/\text{cm}^2$. The power density $0.18 \text{ W}/\text{cm}^2$ would correspond to 5.74×10^{17} photons/s cm^2 . When the device is at 2.0 V, the current density is $0.71 \text{ A}/\text{cm}^2$, which corresponds to 4.34×10^{18} electrons/s cm^2 . Assuming that the quantum efficiency is 1.0 for PL, the results suggest that only about 13% of the injected electrons would accumulate at the GaSb/GaAs interface and undergo optical recombination. In this case, if the fitting curve equation for PL peak energies is to be applied to EL peak energies, the equation should be modified to as (EL peak energy) = $1.04648 + 0.05673 (0.13 \times \text{power density})^{1/3}$. To obtain a better fitting over the experimental data, the y-axis intercept is changed to 1.05648 eV. The fitting curve and the experimental EL peak energies are shown in Fig. 3. As shown in the figure, good agreement between the fitting curve (EL peak energy) = 1.05648

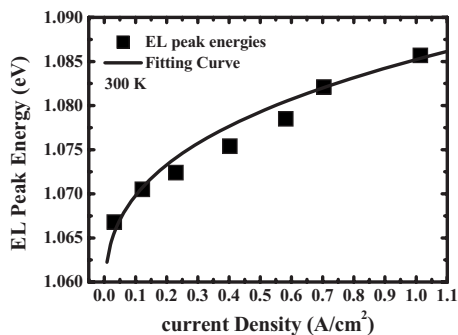


FIG. 3. The EL peak energies of the device under different injection current densities and the fitting curve following the same function with minor modifications for PL peaks.

+0.05673 (0.13 × power density)^{1/3} and the EL peak energies is observed. The phenomenon suggests that compared with PL measurements, a 10 meV higher peak energy is obtained for EL measurements under the same excitation condition. Possible mechanism responsible for this phenomenon may be the steepened triangular well in the GaAs region induced by the forward applied voltages.

To explain the EL mechanisms of the type-II GaSb/GaAs QD structures, schematic band diagrams of the device with forward applied voltages larger than the turn-on voltage 0.8 V is shown in Fig. 4. As shown in the figure, when the device turns on, the electrically injected holes in the GaSb QDs would induce a triangular well in the GaAs region. Therefore, the injected electrons would tend to accumulate at the GaAs/GaSb interface. In this case, although separate confinements for electrons and holes are obtained for the type-II heterostructure, the overlap of wave functions is not negli-

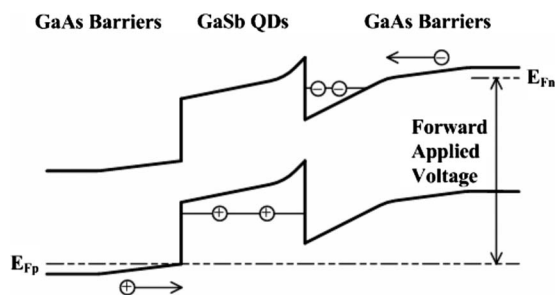


FIG. 4. Schematic band diagram of the device with forward applied voltages larger than the turn-on voltage 0.8 V.

gible such that dipole transition probability would greatly increase. The results would be an observable EL signal when the device turns on. As shown in the figure, the low efficiency of injected carriers for optical recombination could be improved by inserting high-bandgap carrier confinement layers such as AlGaAs before and after the GaSb/GaAs QD structure.

In conclusion, a GaSb/GaAs QD LED with a single GaSb QD layer is investigated. Significant EL is observed for the device under forward biases, which suggests that pronounced dipole transitions occur at the GaSb/GaAs interfaces. With increasing forward biases, the observed EL peak blue shift confirms that the origin of luminescence is from the type-II GaSb/GaAs QD structures. The linear dependence of PL and EL peaks over the third root of the excitation densities has confirmed that the type-II GaSb/GaAs QDs should be responsible for the luminescence. The wide barrier choices from GaAs, GaAsSb to InGaP of this material system have provided an alternate approach for infrared light-emitting devices.

This work was supported in part by the National Science Council, Taiwan under Grant Nos. NSC 98-2221-E-001-001 and NSC 99-2911-I-001-010.

- ¹F. Heinrichsdorff, M.-H. Mao, N. Kirstaedter, A. Krost, D. Bimberg, A. O. Kosogov, and P. Werner, *Appl. Phys. Lett.* **71**, 22 (1997).
- ²H. Y. Liu, D. T. Childs, T. J. Badcock, K. M. Groom, I. R. Sellers, M. Hopkinson, R. A. Hogg, D. J. Robbins, D. J. Mowbray, and M. S. Skolnick, *IEEE Photon. Technol. Lett.* **17**, 1139 (2005).
- ³W. H. Lin, K. P. Chao, C. C. Tseng, S. C. Mai, S. Y. Lin, and M. C. Wu, *J. Appl. Phys.* **106**, 054512 (2009).
- ⁴S. Y. Lin, W. H. Lin, C. C. Tseng, K. P. Chao, and S. C. Mai, *Appl. Phys. Lett.* **95**, 123504 (2009).
- ⁵W. S. Liu, H. Chang, Y. S. Liu, and J. I. Chyi, *J. Appl. Phys.* **99**, 114514 (2006).
- ⁶W. S. Liu, D. M. T. Kuo, J. I. Chyi, W. Y. Chen, H. S. Chang, and T. M. Hsu, *Appl. Phys. Lett.* **89**, 243103 (2006).
- ⁷G. Balakrishnan, J. Tatebayashi, A. Khoshkhalagh, S. H. Huang, A. Jallipalli, L. R. Dawson, and D. L. Huffaker, *Appl. Phys. Lett.* **89**, 161104 (2006).
- ⁸M.-C. Lo, S.-J. Huang, C.-P. Lee, S.-D. Lin, and S.-T. Yen, *Appl. Phys. Lett.* **90**, 243102 (2007).
- ⁹F. Hatami, M. Grundmann, N. N. Ledentsov, F. Heinrichsdorff, R. Heitz, J. Böhrer, D. Bimberg, S. S. Ruvimov, P. Werner, V. M. Ustinov, P. S. Kop'ev, and Zh. I. Alferov, *Phys. Rev. B* **57**, 4635 (1998).
- ¹⁰T. Nakai, S. Iwasaki, and K. Yamaguchi, *Jpn. J. Appl. Phys., Part 1* **43**, 2122 (2004).
- ¹¹D. Alonso-Álvarez, B. Alén, J. M. García, and J. M. Ripalda, *Appl. Phys. Lett.* **91**, 263103 (2007).